Phosphodiester Hydrolysis by a New Zinc(II) Macrocyclic Tetraamine Complex with an Alcohol Pendant: Elucidation of the Roles of Ser-102 and Zinc(II) in Alkaline Phosphatase

Eiichi Kimura,*,† Yorimitsu Kodama,† Tohru Koike,† and Motoo Shiro‡

Contribution from the Department of Medicinal Chemistry, School of Medicine, Hiroshima University, Kasumi 1-2-3, Minami-ku, Hiroshima 734, Japan, and Rigaku Corporation, Matsubaracho 3-9-12, Akishima, Tokyo 196, Japan

Received March 28, 1995®

Abstract: A new benzyl alcohol-pendant 1,4,7,10-tetraazacyclododecane (cyclen) ligand, (*S*)-1-(2-hydroxy-2-phenylethyl)-1,4,7,10-tetraazacyclododecane (L) (**11**), has been synthesized. The complexation of **11** with Zn^{II} yielded 1:1 five-coordinate complexes (isolated as its perchlorate salts with the pendant alcohol either undissociated (ZnL, **14a**) or dissociated ($ZnH_{-1}L$, **14b**) from acidic (pH 6.0) or basic (pH 9.5) aqueous solution, respectively). The pK_a value for the pendant alcohol (**14a** ⇌ **14b** + H^+) was determined by potentiometric pH titration to be 7.30 ± 0.02 at 35 °C with $I = 0.10$ ($NaNO_3$). The X-ray crystal study of **14b** has shown two crystallographically distinct structures with the alkoxide closely coordinated at the fifth coordination site, where an average distance of Zn−O^- is 1.91 Å. Crystals of **14b**·ClO_4 ($C_{16}H_{27}N_4O_5ClZn$) are orthorhombic, space group $P2_12_12_1$ (no. 19) with a = 16.977 (4) Å, b = 18.135 (4) Å, c = 13.173 (3) Å, V = 4055 (1) Å^3, Z = 8, R = 0.050, and R_w = 0.077. The Zn^{II}-bound alkoxide anion in **14b** is a more reactive nucleophile than *N*-methylcyclen-Zn^{II}−OH^- species **15b**. In the kinetic study using **14** in aqueous solution (pH 6.0−10.3) at 35 °C with $I = 0.10$ ($NaNO_3$), the rate−pH profile for a phosphoryl transfer reaction from bis(4-nitrophenyl) phosphate (BNP^-) to **14b** gave a sigmoidal curve with an inflection point at pH 7.4, which corresponds to the pK_a value for **14a** ⇌ **14b** + H^+. The second-order rate constant k_{BNP} of (6.5 ± 0.1) × 10^{-4} M^{-1} s^{-1} is 125 times greater than the corresponding value of (5.2 ± 0.2) × 10^{-6} M^{-1} s^{-1} for BNP^- hydrolysis catalyzed by **15b**. The product of the phosphoryl transfer reaction from BNP^- to **14b** is the pendant alcohol-phosphorylated **16**, which was isolated as its perchlorate salt **16a** by reacting **14b** with BNP^- in DMF. In anhydrous DMF solution, the phosphoryl transfer (k_{BNP} of 1.1 ± 0.1 M^{-1} s^{-1} at 35 °C) is 1700 times faster than that in aqueous solution. In the subsequent reaction of **16**, the pendant phosphodiester undergoes an intramolecular nucleophilic attack by the Zn^{II}-bound OH^- of **16b** to yield a phosphomonoester product **17**. From the sigmoidal rate−pH relationship (pH 7.4−10.5), the kinetic pK_a value of 9.0 was estimated for **16a** ⇌ **16b** + H^+, which is almost the same value (pK_a = 9.10 ± 0.05) determined by potentiometric pH titration at 35 °C. The first-order rate constant for the reaction **16b** → **17** is (3.5 ± 0.1) × 10^{-5} s^{-1} at 35 °C with I = 0.10 ($NaNO_3$). As a reference to this intramolecular phosphodiester hydrolysis, ethyl (4-nitrophenyl) phosphate (NEP^-) was hydrolyzed by **15b**. The second-order rate constant k_{NEP} was (7.9 ± 0.3) × 10^{-7} M^{-1} s^{-1} at 35 °C with I = 0.10 ($NaNO_3$). Thus, the intramolecular hydrolysis is 45 000 times faster than the intermolecular NEP^- hydrolysis with 1 mM **15b**. The present findings that demonstrate the potential of the proximate alcohol by Zn^{II} in the initial phosphoryl transfer and the potential of the Zn^{II}-bound water in the intramolecular phosphate hydrolysis may well serve to elucidate the collaborative functions of Ser-102 and Zn^{II} ions in alkaline phosphatase.

Introduction

Alkaline phosphatase (AP) is a Zn^{II}-containing enzyme that nonspecifically hydrolyzes phosphate monoesters ($ROPO_3^{2-}$) at alkaline pH.[1] Intensive studies have been done on *E. coli* alkaline phosphatase. On the basis of X-ray structure[2] and NMR study[3] of native and metallo-substituted AP, it is now accepted that, at the AP active center consisting of two Zn^{II} ions (ca. 4 Å separation), a substrate monophosphate is initially attacked by Ser-102 in **1** to yield a phosphoseryl−enzyme intermediate **2**, which subsequently is attacked by the adjacent Zn^{II}−OH^- to complete the hydrolysis **3** → **4** and reproduce the free form of serine to reinitiate the catalytic cycle (see Scheme 1).[4]

In Scheme 1, the A-site Zn^{II} serves to coordinate the phosphate substrate to make it vulnerable to the attack of Ser-102 that is potentiated by the B-site Zn^{II} (**1**). After the phosphate is transferred from the substrate to Ser-102 (**2**), the vacated coordination site of the A-site Zn^{II} activates an H_2O as Zn^{II}−OH^-, which becomes an intramolecular nucleophile in the final dephosphorylation (**3** → **4**). The wild-type AP reaches maximal activity around pH 8, where the rate-limiting step is release of the tightly bound inorganic phosphate (the product) from the enzyme−product complex **4**. Accordingly, inorganic phosphate is a competitive inhibitor. At pH < 5.5, the phosphoseryl intermediate **2** is stable.[3d,5]

There are some intrinsic questions concerning the AP mechanism, such as (i) what is the special advantage in forming the phosphoseryl intermediate **2** for indirect hydrolysis and (ii) how does the Ser-102 associated with the Zn^{II} ion become a nucleophile? Recently, the Ser-102 in AP was replaced using site-directed mutagenesis by Leu and Ala.[6] The mutant enzymes still catalyzed the phosphate hydrolysis, with similar rate−pH

† Hiroshima University.
‡ Rigaku Corp.
® Abstract published in *Advance ACS Abstracts,* August 1, 1995.

(1) Coleman, J. E. *Annu. Rev. Biophys. Biomol. Struct.* **1992**, *21*, 441−483.
(2) Kim, E. E.; Wyckoff, H. W. *J. Mol. Biol.* **1991**, *218*, 449−464.
(3) (a) Gettins, P.; Coleman, J. E. *J. Biol. Chem.* **1984**, *259*, 4991−4997. (b) Hull, W. E.; Halford, S. E.; Gutfreund, H.; Sykes, B. D. *Biochemistry* **1976**, *15*, 1547−1561. (c) Bock, J. L.; Cohn, M. *J. Biol. Chem.* **1978**, *253*, 4082−4085. (d) Coleman, J. E.; Gettins, P. *Zinc Enzymes*; Birkhäuser: Boston, MA, 1986; Chapter 6, p 77.
(4) For a review: Fenton, D. E.; Okawa, H. *J. Chem. Soc., Dalton Trans.* **1993**, 1349−1357.
(5) Ried, T. W.; Wilson, L. B. *Enzyme* **1971**, *4*, 373−415.

0002-7863/95/1517-8304$09.00/0

Scheme 1

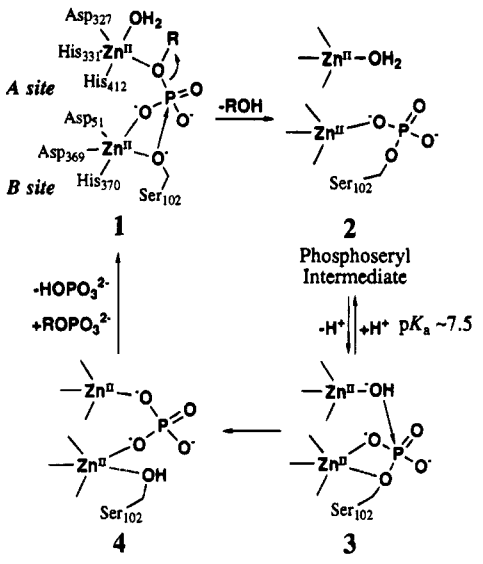

Alkaline Phosphatase Active Center

profiles, although the catalytic efficiency is 1/500 to 1/1000 of that of the wild-type enzyme, for which the direct hydrolysis of the substrate by $Zn^{II}-OH^-$ was proposed. In other hydrolytic metalloenzymes, the direct hydrolysis by $M-OH^-$ species seems more prevalent.[7]

There have been numerous studies of phosphatase model systems using simple metal complexes,[8,9] but most of these models have been built for *the sole $M-OH^-$ systems as nucleophiles, while few were concerned with the net reaction initiated by the metal-bound alcohol, followed by the metal-bound water, as was revealed by AP.*

Recently, we discovered that Zn^{II}–1,5,9-triazacyclododecane ([12]aneN$_3$) complex **5a**[10,11] and Zn^{II}–1,4,7,10-tetraazacyclododecane (cyclen) complex **6a**[12] can activate an H_2O as the Zn^{II}-bound OH^- species **5b** (pK_a = 7.3) and **6b** (pK_a = 7.9) and that both catalyze hydrolysis of carboxyesters,[10a–c] β-lactams,[12] phosphotriesters, and phosphodiesters.[10c] We further disclosed that the alcohol-pendant *N*-hydroxyethyl on [12]aneN$_3$ and cyclen formed 1:1 Zn^{II} complexes **7**[13] and **8**,[14] which more efficiently catalyze 4-nitrophenyl acetate hydrolysis. These were the novel models of metallocatalysts that *indirectly* hydrolyze the carboxyl ester via the rate-limiting "*acyl intermediates*" **9** and **10**, respectively. Using **8** and bis(4-nitrophenyl) phosphate

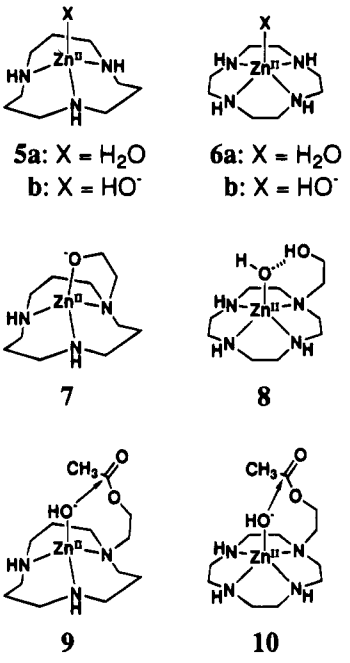

(BNP$^-$), we also checked the phosphatase activity in aqueous solution. The phosphoryl transfer reaction from BNP$^-$ to **8** could be followed as 4-nitrophenolate production,[15] but the following reaction was too complex to allow the elucidation of the total reaction mechanism.

In this study, we synthesized a new benzyl alcohol-pendant cyclen **11**, bearing a chiral carbon adjacent to the phenyl group. We have discovered that **11** yields a 1:1 Zn^{II} complex whose phosphoester bond cleavage activity has a very distinct reaction mechanism. We herein describe a novel chemical model for Zn^{II}-involving serine enzymes as part of our series of studies on the intrinsic chemical properties of Zn^{II} in alkaline phosphatase. We also attempted the enantioselective hydrolysis of various carboxyesters with **11**, which will be reported elsewhere.

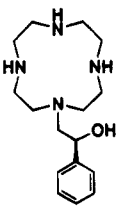

11

(6) Butler-Ransohoff, J. E.; Rokita, S. E.; Kendall, D. A.; Banzon, J. A.; Carano, K. S.; Kaiser, E. T.; Matlin, A. R. *J. Org. Chem.* **1992**, *57*, 142–145.

(7) (a) Mueller, E. G.; Crowder, M. W.; Averill, B. A.; Knowles, J. R. *J. Am. Chem. Soc.* **1993**, *115*, 2974–2975. (b) Coleman, J. E. *Zinc Enzymes*; Birkhäuser: Boston, MA, 1986; Chapter 4, p 49.

(8) For a review of bimetallic enzyme models: (a) Göbel, M. W. *Angew. Chem., Int. Ed. Engl.* **1994**, *33*, 1141–1143. (b) Karlin, K. D. *Science* **1993**, *261*, 701–708.

(9) (a) For Ir^{III} complexes: Hendry, P.; Sargeson, A. M. *J. Am. Chem. Soc.* **1989**, *111*, 2521–2527. (b) For Co^{III} complexes: Jones, D. R.; Lindoy, L. F.; Sargeson, A. M. *J. Am. Chem. Soc.* **1983**, *105*, 7327–7336. Hendry, P.; Sargeson, A. M. *Inorg. Chem.* **1990**, *29*, 92–97. Chin, J.; Banaszczyk, M.; Jubian, V.; Zou, X. *J. Am. Chem. Soc.* **1989**, *111*, 186–190. Kim, J. H.; Chin, J. *J. Am. Chem. Soc.* **1992**, *114*, 9792–9795. Connolly, J. A.; Banaszczyk, M.; Hynes, R. C.; Chin, J. *Inorg. Chem.* **1994**, *33*, 665–669. (c) For Ln^{III} complexes: Schneider, H.-J.; Rammo, J.; Hettich, R. *Angew. Chem., Int. Ed. Engl.* **1993**, *32*, 1716–1719. Hay, R. W.; Govan, N. *J. Chem. Soc., Chem. Commun.* **1990**, 714–715. Morrow, J. R.; Buttrey, L. A.; Shelton, V. M.; Berback, K. A. *J. Am. Chem. Soc.* **1992**, *114*, 1903–1905. Chin, K. O. A.; Morrow, J. R. *Inorg. Chem.* **1994**, *33*, 5036–5041. Tsubouchi, A.; Bruice, T. C. *J. Am. Chem. Soc.* **1994**, *116*, 11614–11615. (d) For Zn^{II} complexes: Sigman, D. S.; Jorgensen, C. T. *J. Am. Chem. Soc.* **1972**, *94*, 1724–1731. Gellman, S. H.; Petter, R.; Breslow, R. *J. Am. Chem. Soc.* **1986**, *108*, 2388–2394. Hikichi, S.; Tanaka, M.; Moro-oka, Y.; Kitajima, N. *J. Chem. Soc., Chem. Commun.* **1992**, 814–815. Ruf, M.; Weis, K.; Vahrenkamp, H. *J. Chem. Soc., Chem. Commun.* **1994**, 135–136. (e) For Fe^{III} complexes: Wilkinson, E. C.; Dong, Y.; Que, L. Jr. *J. Am. Chem. Soc.* **1994**, *116*, 8394–8395.

(10) (a) Kimura, E.; Shiota, T.; Koike, T.; Shiro, M.; Kodama, M. *J. Am. Chem. Soc.* **1990**, *112*, 5805–5811. (b) Kimura, E.; Koike, T.; Shionoya, M.; Shiro, M. *Chem. Lett.* **1992**, 787–790. (c) Koike, T.; Kimura, E. *J. Am. Chem. Soc.* **1991**, *113*, 8935–8941. (d) Zhang, X.; van Eldik, R.; Koike, T.; Kimura, E. *Inorg. Chem.* **1993**, *32*, 5749–5755. (e) Koike, T.; Kimura, E.; Nakamura, I.; Hashimoto, Y.; Shiro, M. *J. Am. Chem. Soc.* **1992**, *114*, 7338–7345. (f) Kimura, E.; Shionoya, M.; Hoshino, A.; Ikeda, T.; Yamada, Y. *J. Am. Chem. Soc.* **1992**, *114*, 10134–10137.

(11) (a) Kimura, E.; Koike, T. *Comments Inorg. Chem.* **1991**, *11*, 285–301. (b) Kimura, E. In *Progress in Inorganic Chemistry*; Karlin, K. D., Ed.; John Wiley & Sons: New York, 1994; Vol. 41, 443–492.

(12) Koike, T.; Takamura, M.; Kimura, E. *J. Am. Chem. Soc.* **1994**, *116*, 8443–8449.

(13) Kimura, E.; Nakamura, I.; Koike, T.; Shionoya, M.; Kodama, Y.; Ikeda, T.; Shiro, M. *J. Am. Chem. Soc.* **1994**, *116*, 4764–4771.

(14) Koike, T.; Kajitani, S.; Nakamura, I.; Kimura, E.; Shiro, M. *J. Am. Chem. Soc.* **1995**, *117*, 1210–1219.

(15) The second-order rate constant for the 4-nitrophenolate release reaction from BNP$^-$ with **8** (determined by initial slop method) is (5.0 ± 0.1) × 10^{-4} M^{-1} s^{-1} in aqueous solution at 35 °C with I = 0.10 ($NaNO_3$). Kimura, E.; Koike, T. Unpublished results.

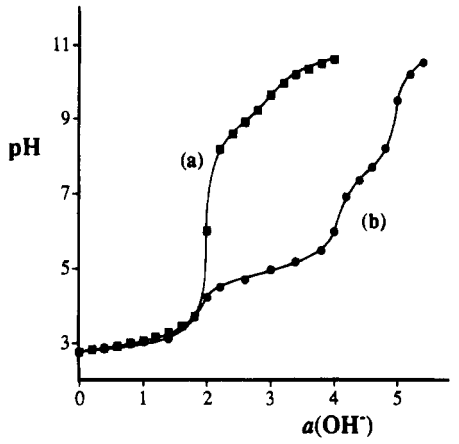

Figure 1. Typical titration curves for **11** at 25 °C with I = 0.10 ($NaClO_4$): (a) 1.0 mM of **11**·4HCl; (b) a + 1.0 mM $ZnSO_4$.

Scheme 2

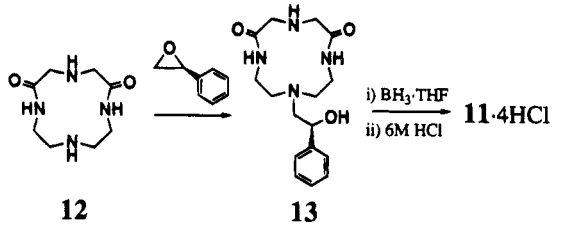

Results and Discussion

Synthesis of (*S*)-1-(2-Hydroxy-2-phenylethyl)-1,4,7,10-tetraazacyclododecane (Benzyl Alcohol-Pendant Cyclen, 11) (Scheme 2). The macrocyclic dioxotetraamine **12**[16] and (*S*)-styrene oxide were heated to reflux in EtOH for 1 day to obtain (*S*)-1-(2-hydroxy-2-phenylethyl)-5,9-dioxo-1,4,7,10-tetraazacyclododecane (**13**) in 46% yield. Both amide groups were reduced with BH_3−THF complex in THF to give (*S*)-1-(2-hydroxy-2-phenylethyl)-1,4,7,10-tetraazacyclododecane (**11**), which was isolated as its tetrahydrochloride salt from 6 M HCl aqueous solution in 62% yield. Using *rac*-styrene oxide as the starting material, the corresponding racemic ligand was yielded in 24%. For all the following studies, we used the enantiomeric product **11**.

Protonation and Zinc(II) Complexation Constants of the Benzyl Alcohol-Pendant Cyclen (11). The protonation constants (K_n) of **11** were determined by potentiometric pH titrations of **11**·4HCl (1 mM) using 0.10 M NaOH with I = 0.10 ($NaClO_4$) at 25 °C. A typical pH titration curve is shown in Figure 1a. The titration data were analyzed for equilibria 1−4. The mixed protonation constants K_1−K_4 (a_{H^+} is the activity of H^+) are defined as follows:

$$L + H^+ \rightleftharpoons HL \qquad K_1 = [HL]/[L]a_{H^+} \qquad (1)$$

$$HL + H^+ \rightleftharpoons H_2L \qquad K_2 = [H_2L]/[HL]a_{H^+} \qquad (2)$$

$$H_2L + H^+ \rightleftharpoons H_3L \qquad K_3 = [H_3L]/[H_2L]a_{H^+} \qquad (3)$$

$$H_3L + H^+ \rightleftharpoons H_4L \qquad K_4 = [H_4L]/[H_3L]a_{H^+} \qquad (4)$$

Table 1 summarizes the obtained protonation constants (log K_n) in comparison with the reported K_n values of cyclen and *N*-(hydroxyethyl)cyclen (HE-cyclen) under the same conditions. The K_1 and K_2 values of **11** are extremely large with respect to K_3 and K_4 values, which are roughly the same as those of cyclen and HE-cyclen.

(16) Kimura, E.; Kuramoto, Y.; Koike, T.; Fujioka, H.; Kodama, M. *J. Org. Chem.* **1990**, *55*, 42−46.

Table 1. Comparison of the Protonation Constants of Cyclen Ligands and Zn^{II} Complexation Constants[a]

	11	cyclen	HE-cyclen	methylcyclen
log K_1	10.92 ± 0.05[b]	11.04[c]	10.72[c]	
log K_2	8.87 ± 0.03[b]	9.86[c]	9.28[c]	
log K_3	<2[b]	<2[c]	<2[c]	
log K_4	<2[b]	<2[c]	<2[c]	
log K(ZnL)	13.6 ± 0.1[d]	15.3[c]	13.8[c]	15.1[e]
pK_a				
25 °C	7.51 ± 0.02[f]	7.86[g]	7.60[h]	7.68[e]
35 °C	7.30 ± 0.02[i]	7.64[g]	7.41[h]	7.50 ± 0.02[j]

[a] K_n = $[H_nL]/[H_{n-1}L]a_{H^+}$. K(ZnL) = [ZnL]/[L][Zn^{II}]. pK_a = −log($[ZnH_{-1}L]a_{H^+}$/[ZnL]). [b] At 25 °C with I = 0.10 ($NaClO_4$). [c] From ref 14 at 25 °C with I = 0.10 ($NaClO_4$). [d] Determined with 1.0 mM of **14a** and 4 equiv of $HClO_4$ at 25 °C with I = 0.10 ($NaClO_4$). [e] From ref 17 at 25 °C with I = 0.10 ($NaClO_4$). [g] From ref 12 with I = 0.10 ($NaClO_4$). [h] From ref 14 with I = 0.10 ($NaClO_4$). [i] Determined with 1.0 mM of **14a** and I = 0.10 ($NaNO_3$). [j] Determined with 1.0 mM of **15a** and I = 0.10 ($NaNO_3$).

Scheme 3

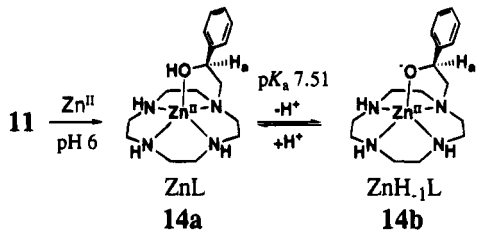

The potentiometric pH titration curve of **11**·4HCl in the presence of an equimolar amount of Zn^{II} using 0.10 M NaOH (Figure 1b) revealed two distinct equilibria: the first is the ZnL complex formation at 4 < pH < 6 until a = 4, and the second is monodeprotonation from ZnL (4 < a < 5). Up to a = 4, the equilibration was extremely slow, so that we had to wait more than 2 h for each titration point. The titration data were treated for the 1:1 ZnL (**14a**) complex (eq 5) and its monodeprotonated complex $ZnH_{-1}L$ (**14b**) (eq 6),

$$L + Zn^{II} \rightleftharpoons ZnL \qquad K(ZnL) = [ZnL]/[L][Zn^{II}] \qquad (5)$$

$$ZnL \rightleftharpoons ZnH_{-1}L + H^+ \qquad K_a = [ZnH_{-1}L]a_{H^+}/[ZnL] \qquad (6)$$

where $H_{-1}L$ denotes alcoholic OH-deprotonated ligand (Scheme 3). The obtained values log K(ZnL) at 25 °C and deprotonation constants pK_a at 25 and 35 °C and listed in Table 1. Any further deprotonation or precipitation of $Zn(OH)_2$ was not observed over pH 12, indicating the monodeprotonated species to be stable until pH ca. 12. The deprotonation constants pK_a (eq 6) of 7.51 ± 0.02 and 7.30 ± 0.02 determined by the pH-metric titration respectively at 25 °C with I = 0.10 ($NaClO_4$) and 35 °C with I = 0.10 ($NaNO_3$) are near those of **6a**[12] and Zn^{II}−*N*-methylcyclen **15a**[17](see Table 1). Fortunately, both the ZnL

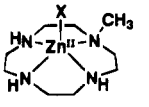

15a: X = H_2O
b: X = HO^-

(**14a**) and $ZnH_{-1}L$ (**14b**) complexes were crystallized as their

(17) Shionoya, M.; Ikeda, T.; Kimura, E.; Shiro, M. *J. Am. Chem. Soc.* **1994**, *116*, 3848−3859. The Zn^{II} complexation constant log K(ZnL) for **15a** is 15.1 ± 0.1 at 25 °C with I = 0.10 ($NaClO_4$). Kimura, E.; Ikeda, T. Unpublished results.

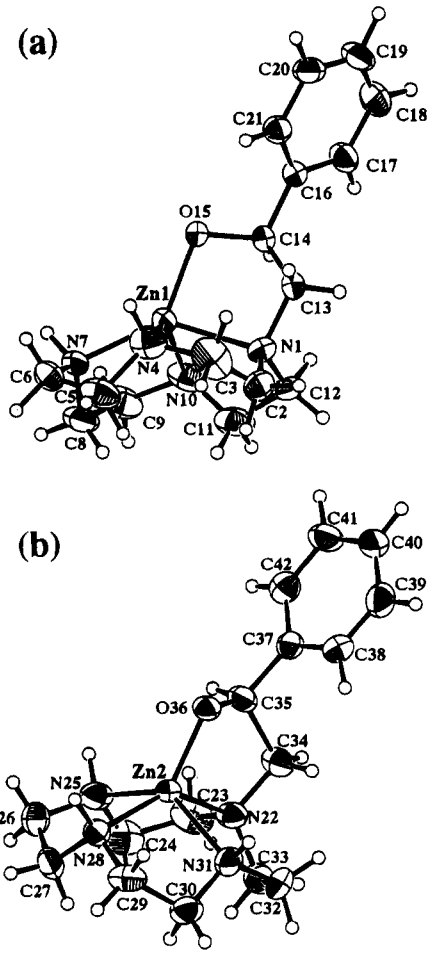

Figure 2. ORTEP drawing (30% probability ellipsoids) of the two crystallographically distinct molecules (a and b) of **14b**·ClO_4. ClO_4 anions were omitted for clarity. Bond distances: (a) Zn(1)–O(15) 1.915(5), Zn(1)–N(1) 2.172(7), Zn(1)–N(4) 2.173(8), Zn(1)–N(7) 2.067(7), Zn(1)–N(10) 2.143(8) Å; (b) Zn(2)–N(22) 2.155(7), Zn-(2)–N(25) 2.161(8), Zn(2)–N(28) 2.056(7), Zn(2)–N(31) 2.169(7) Å. Bond angles: (a) N(1)–Zn(1)–N(4) 81.2(3), N(1)–Zn(1)–N(10) 81.4-(4), N(4)–Zn(1)–N(7) 84.0(4), N(7)–Zn(1)–N(10) 82.2(4), O(15)–Zn(1)–N(1) 86.8(2)°; (b) N(22)–Zn(2)–N(25) 82.8(4), N(22)–Zn(2)–N(31) 80.6(3), N(25)–Zn(2)–N(28) 82.1(3), N(28)–Zn(2)–N(31) 82.8(3), O(36)–Zn(2)–N(22) 86.7(2)°.

perchlorate salts from pH 6 and 9.5 aqueous solutions, respectively. The structure of the monodeprotonated complex **14b** was confirmed by the X-ray crystal analysis (vide infra). As the solution pH became higher, the chemical shifts of the benzyl proton H_a for **14** moved upfield from δ 5.14 at pD 6.0 (**14a**) to δ 4.86 at pD > 9.5 (**14b**). From these facts and the following results, we assigned the deprotonated structure to be **14b** rather than Zn^{II}–OH^- species in aqueous alkaline solution.

X-ray Crystal Structure of the Zn^{II} Complex of the Deprotonated Benzyl Alcohol-Pendant Cyclen (14b). When the benzyl alcohol-pendant cyclen **11** (in the acid-free form L, see the Experimental Section) in water was mixed with 1 equiv of $Zn^{II}(ClO_4)_2 \cdot 6H_2O$ at 60 °C, **14a**·$(ClO_4)_2$ was obtained as colorless crystals. Addition of 1 equiv of NaOMe to **14a**·$(ClO_4)_2$ in MeOH gave **14b**·ClO_4, which was recrystallized from aqueous alkaline solution (pH 9.5).

Figure 2 shows an ORTEP drawing of **14b**·ClO_4 with 30% probability thermal ellipsoids. Selected crystal data and collection parameters are displayed in Table 2. In this Zn^{II} complex, there are two crystallographically distinct molecules (Figure 2a,b). The Zn^{II} ions Zn_1 and Zn_2, respectively, lie above the four nitrogen atoms (N_1, N_4, N_7, N_{10} and N_{22}, N_{25}, N_{28}, N_{31}), and are apically bound with the pendant alkoxide oxygens O_{15} and O_{36}, respectively. The angles N_1–Zn_1–N_7 and N_{22}–Zn_2–N_{28} and N_4–Zn_1–N_{10} and N_{25}–Zn_2–N_{31} are respectively bent at 138.5 and 139.2° and 135.0 and 134.5°, indicating distorted tetragonal-pyramidal structures. The average Zn–O^- bond distance of 1.91 Å is much shorter than the Zn–N bonds (2.056–2.173 Å). The Zn–O^- distance is shorter in the Zn^{II}–anion donor than in other Zn^{II}–macrocyclic polyamine complexes.[10b,13,14,18] The earlier Zn–O bond distance with the neutral alcohol pendant in **8** was 1.994 Å.[14] The apical Zn–O^- bond is bent with the N_1–Zn_1–O_{15} and N_{22}–Zn_2–O_{36} angles of 86.8 and 86.7°, respectively. One may view **14b** as having a distorted trigonal-bipyramidal structure with N_1, N_7, and O_{15} as equatorial donors and N_4 and N_{10} as axial donors.

Although the pendant alkoxide donor binds firmly with Zn^{II} in the solid state, this bonding would be kinetically labile in DMF and H_2O solutions, so that this alkoxide anion can be a good nucleophile for the phosphoryl transfer reaction with BNP^-.

Net Reaction of the Benzyl Alcohol-Pendant Cyclen–Zn^{II} Complex 14b with Bis(4-nitrophenyl) Phosphate (BNP^-). The $ZnH_{-1}L$ complex **14b** has been tested as a simplified model of AP. Since the phosphomonoester (e.g., 4-nitrophenyl phosphate (NPP^{2-})) was hydrolyzed impractically slowly, we used a more reactive substrate, phosphodiester bis(4-nitrophenyl) phosphate (BNP^-).

The overall reaction of BNP^- (25 mM) with **14b** (20 mM) was followed by the ^1H NMR of the benzyl protons in D_2O at 35 °C and pD = 10.3 (0.1 M CHES buffer) (see Figure 3). The

Table 2. Selected Crystallographic Data for **14b**·ClO_4

empirical formula	$C_{16}H_{27}N_4O_5ClZn$
formula weight	456.25
crystal color, habit	colorless, prismatic
crystal system	orthorhombic
space group	$P2_12_12_1$ (no. 19)
lattice parameters	a = 16.977(4) Å
	b = 18.135(4) Å
	c = 13.173(3) Å
	V = 4055(1) Å^3
	Z = 8
μ(Cu Kα)	31.96 cm^{-1}
radiation	Cu Kα (λ = 1.541 78 Å) graphite monochromated
scan type	ω–2θ
scan rate (in ω)	16.0 deg/min (five scans)
scan width	(1.42 + 0.30 tan θ)
$2\theta_{max}$	120.2
no. of reflns measd	3414 (total)
refinement	full-matrix least squares
no. of obs ($I > 3.00\sigma(I)$)	2862
residuals: R; R_w	0.050; 0.077

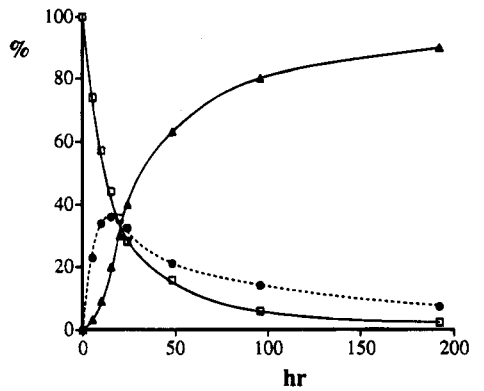

Figure 3. Time course of the relative concentrations of Zn^{II} complexes **14b** (open square), **16** (solid circle), and **17** (solid trigone) for the reaction of BNP^- (25 mM) with **14b** (20 mM) in D_2O at 35 °C, I = 0.10 ($NaNO_3$), and pD = 10.3 (0.1 M CHES buffer). The relative concentrations (%) are based on the initial concentration of **14b**.

(18) Kimura, E.; Koike, T.; Toriumi, K. *Inorg. Chem.* **1988**, *27*, 3687–3688.

Scheme 4

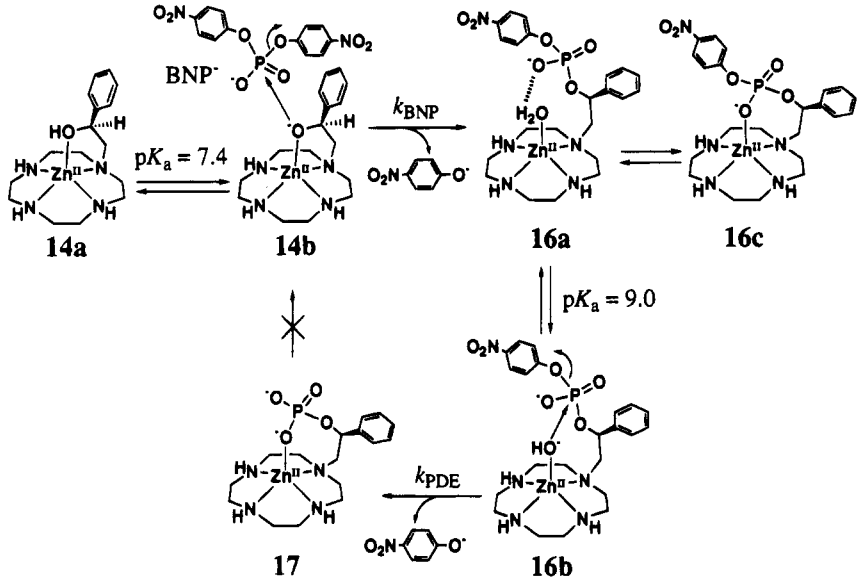

Table 3. Comparison of the Phosphodiester Bond Cleavage Rate Constants, k_{BNP} (M^{-1} s^{-1}), for **14b**, **8**, **15b**, **5b**, and **6b**, and Aqueous OH^- Ion in Aqueous Solution

catalyst	k_{BNP}	catalyst	k_{BNP}
14b	$(6.5 \pm 0.1) \times 10^{-4}$ [a]	**5b**	8.5×10^{-5} [b]
8	5.0×10^{-4} [c]	**6b**	2.1×10^{-5} [b]
15b	$(5.2 \pm 0.2) \times 10^{-6}$ [d]	OH^-(aq)	2.4×10^{-5} [b]

[a] Determined with 2.0, 1.0, and 0.5 mM **14b** and 10, 5.0, and 2.5 mM BNP^- at 35 °C with $I = 0.10$ ($NaNO_3$). [b] From ref 10c at 35 °C with $I = 0.20$ ($NaClO_4$). [c] From ref 15 at 35 °C with $I = 0.10$ ($NaNO_3$). [d] Determined with 16, 8.0, and 4.0 mM **14b** and 10, 5.0, and 2.5 mM BNP^- at 35 °C with $I = 0.10$ ($NaNO_3$).

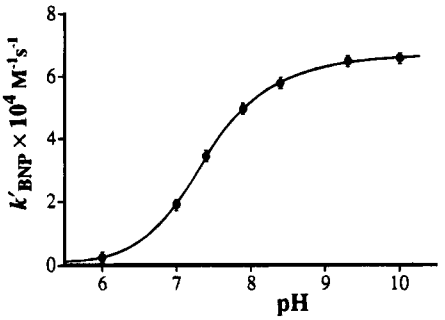

Figure 4. Rate–pH profile for the second-order rate constants of the phosphoryl transfer from BNP^- to **14** (see eq 7) at 35 °C with I = 0.10 ($NaNO_3$) in aqueous solution.

initial product **16** (a new triplet at δ 5.56), which later was proven to be the phosphoryl intermediate, increased as the starting **14b** (δ 4.83) decreased. The final product **17** (δ 5.90, see blow) appeared subsequently. After 192 h, **14b** and **16** diminished to 2.5% and 7.5%, respectively, and the majority (90%) of the initial Zn^{II} complex was converted to **17**, where almost 2 equiv of 4-nitrophenolate was released (191% based on initial concentration of **14b**). The same reaction was followed by ^{31}P NMR under the same conditions, and the products **16** and **17** were identified as δ −5.7 and 5.9, respectively. No other side product was detected. We assigned the net reaction scheme as depicted in Scheme 4, with the aid of the following results.

A Kinetic Study of the Initial Reaction 14b → 16. The initial phosphorylation rate in aqueous solution at 35 °C, I = 0.10 ($NaNO_3$), and pH 6.0–10.3 (20 mM Good's buffer) was followed by the appearance of 4-nitrophenolate at 400 nm. The second-order dependence of the rate constant k'_{BNP} on the total concentration of Zn^{II} complex (= [**14a**] + [**14b**]) and [BNP^-] fits the kinetic eq 7, where v is the 4-nitrophenolate releasing rate. The second-order rate constant, k'_{BNP} is plotted as a function of pH (see Figure 4). The resulting sigmoidal curve indicates a kinetic process controlled by an acid–base equilibrium. The inflection point at pH 7.4 is almost the same as the pK_a value of **14** for the pendant alcohol deprotonation (eq 6). Therefore, the reactive species is concluded to be the deprotonated complex **14b**. The second-order rate constant k_{BNP} (see eq 8) of $(6.5 \pm 0.1) \times 10^{-4}$ M^{-1} s^{-1} was determined from the maximum k'_{BNP} values.

$$v = k'_{BNP}[\text{total } Zn^{II} \text{ complex}][BNP^-] \quad (7)$$

$$= k_{BNP}[\mathbf{14b}][BNP^-] \quad (8)$$

For a reference, the hydrolysis of the same substrate BNP^- (to NPP^{2-}) with Zn^{II}–*N*-methylcyclen **15** has been determined by the same method. The kinetics followed the second-order dependence on [BNP^-] and [**15b**]. The rate constant is $(5.2 \pm 0.2) \times 10^{-6}$ M^{-1} s^{-1} at 35 °C, I = 0.10 ($NaNO_3$), and pH 9.3 (20 mM CHES buffer), which demonstrates that *the nucleophilic reaction catalyzed by **14b** is 125 times faster than by **15b***. It is understood that *the Zn^{II}–alkoxide anion is a better nucleophile than Zn^{II}–hydroxide anion toward the phosphate substrate,* just as toward 4-nitrophenyl acetate substrate.[13,14] It should be noted, however, that the reaction with Zn^{II}–alkoxide **14b** is a phosphoryl transfer to form a phosphoryl intermediate **16b** (see Scheme 4), as the previously found acyl transfer with **7** and **8**.[13,14] On the other hand, the reaction with **15b** is a hydroylsis that yields NPP^{2-}.

Isolation of the Phosphoryl Intermediate 16a from the BNP^- Reaction with 14b in DMF. The phosphoryl intermediate **16a** was unequivocally determined by independent isolation of **16a**·ClO_4 by the reaction of BNP^- and **14b** in dry DMF. The structure was identified by elemental analysis (C, H, N) and ^1H, ^{13}C, and ^{31}P NMR. The pH-metric titration of **16a** at 35 °C with I = 0.10 ($NaNO_3$) using 0.1 M aqueous NaOH[19] showed the monodeprotonation and its pK_a of 9.10 ± 0.05, which is assigned to **16a** ⇌ **16b**. The pK_a value is higher than 7.50 ± 0.02 for **15a** ⇌ **15b** at the same conditions, which is possibly due to the proximate phosphate anion binding to the

(19) Hence, the pK_a was determined using the titration data before 0.5% hydrolysis of pendant phosphate.

Zn^{II}, see **16c**. The ^{31}P NMR chemical shift of phosphoryl intermediate **16** in D_2O changed from δ −3.6 at pD 6.5 (**16a**) to δ −6.5 at pD 11 (**16b**).

The reaction of BNP^- with **14b** (the isolated monoperchlorate salt was used) in dry DMF at 35 °C was kinetically studied by observing the appearance of 4-nitrophenolate at 430 nm. The second-order rate constant k_{BNP} (= 1.1 ± 0.1 M^{-1} s^{-1}) with respect to [BNP^-] and [**14b**] was obtained. The comparison of the rate constants k_{BNP} in DMF and aqueous solution points out that the Zn^{II}-bound alkoxide nucleophile acts 1700 times more efficiently in this aprotic solvent than in aqueous solution, which is accounted for by less interfering solvations in DMF.[20] This observation suggests that in hydrophobic environments a phosphoryl transfer at the enzyme active center might occur quite effectively.

Spontaneous Hydrolysis of the Pendant Phosphodiester in 16b to a Phosphomonoester 17 by the Intramolecular Zn^{II}−OH^-. The pendant phosphodiester in **16**, the initial phosphorylation product resulting from the phosphotransfer reaction, was found to undergo spontaneous hydrolysis in alkaline aqueous solution to yield a phosphomonoester **17** (see Scheme 4). We failed to isolate **17** as a solid. This reaction was followed by the ^1H and ^{31}P NMR spectral changes. The disappearance of the reactant **16** (5 mM) (δ 5.56 (OCHC), 6.85 and 8.03 (O_2NArH) for ^1H; δ −5.7 for ^{31}P) matched the appearance of the product **17** (δ 5.09 (OCHC) for ^1H; δ 5.9 for ^{31}P) and 4-nitrophenolate (δ 6.53 and 8.06) in D_2O at 35 °C and pD = 10.3 (0.1 M CHES buffer).

The hydrolysis rate (v_2) of the phosphodiester pendant in **16** was followed by UV spectroscopic measurement (at 400 nm) at pH 7.0−10.5 (20 mM Good's buffer), I = 0.10 ($NaNO_3$), and 35 °C. The first-order dependence on the total concentration of **16** (= [**16a**] + [**16b**] + [**16c**]) is consistent with the kinetic eq 9. The first-order rate constants k'_{PDE} are plotted as a function of pH in Figure 5. The sigmoidal curve indicates characteristic of a kinetic process controlled by an acid−base equilibrium and exhibits an inflection point at pH 9.0, which is almost the same as the pK_a value of 9.1 for the coordinate water of **16a**. Therefore, just as all the previous Zn^{II}−OH^- species,[9d,10c] the Zn^{II}−OH^- in **16b** must be a good nucleophile to the intramolecular phosphate. The first-order rate constant k_{PDE} of (3.5 ± 0.1) × 10^{-5} s^{-1} was obtained from the maximum k'_{PDE} (eq 10).

$$v_2 = k'_{PDE}[\text{total ZnL complex } \mathbf{16}] \quad (9)$$

$$= k_{PDE}[\mathbf{16b}] \quad (10)$$

A prolonged (ca. 1 week) alkaline reaction at 35 °C in 0.1 M aqueous NaOD solution did not change the ^{31}P NMR of **17** (δ 5.9), indicating that **17** is inert and undergoes no more hydrolysis. We assign the final product to the intramolecular phosphomonoester coordinating structure **17**. Earlier, we found that the Zn^{II}−cyclen complex **6a** tends to strongly bind to dianionic phosphomonoester, e.g., log K = 3.3 for 1:1 the NPP^{2-}−Zn^{II}−cyclen complex.[14] Treatment of **17** (5 mM)[21] with EDTA (25 mM) in D_2O at pD 10.3 (0.1 M CHES buffer) stripped Zn^{II} to free the ligand showing a singlet ^{31}P signal at δ 4.2.

(20) (a) A second-order rate constant for hydrolysis of 4-nitrophenyl acetate with **14b** in DMF ((1.1 ± 0.1) × 10^2 M^{-1} s^{-1} at 35 °C) is also 350 times greater than the rate in aqueous solution (0.31 ± 0.01 M^{-1} s^{-1} at 35 °C with I = 0.10 ($NaNO_3$)). Kimura, E.; Kodama, Y. Unpublished results. (b) We have given a thought to running the hydrolysis with Zn^{II}−OH^- complex **15b** in dry DMF as a reference reaction. However, we could not isolate **15b** in any of the attempts using various counteranions such as ClO_4^-, PF_6^-, Cl^-, etc. Generation of **15b** in situ makes the reaction more complex and difficult to interpret.

(21) The solution of **17** was prepared by the reaction of **16a** (5 mM) in D_2O at 50 °C and pD 10.3 (0.1 M CHES buffer) for 1 day.

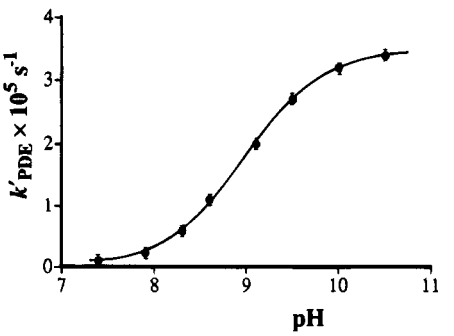

Figure 5. Rate−pH profile for the first-order rate constants of intramolecular phosphodiester hydrolysis of **16** (see eq 9) at 35 °C with I = 0.10 ($NaNO_3$) in aqueous solution.

Scheme 5

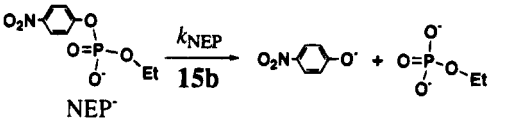

Scheme 6

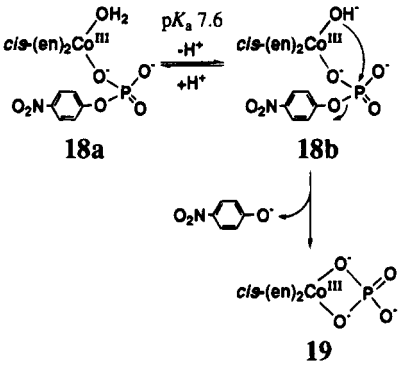

Hydrolysis of Ethyl 4-Nitrophenyl Phosphate (NEP^-) with an Intermolecular Nucleophile Zn^{II}−OH^- 15b (Scheme 5). A Reference Reaction to the Intramolecular Hydrolysis of 16b. In order to see the efficiency of the intramolecular attack of Zn^{II}−OH^- at the pendant phosphodiester in **16b** → **17**, we have measured the rate of an intermolecular reaction between ethyl 4-nitrophenyl phosphate (NEP^-) and (*N*-methylcyclen)−Zn^{II}−OH^- (**15b**) (Scheme 5) under the same conditions. The kinetics, followed by the appearance of 4-nitrophenolate at pH 9.3, showed the second-order rate constant k_{NEP} of (7.9 ± 0.3) × 10^{-7} M^{-1} s^{-1}. One can calculate the effective molarity of 45 M (= k_{PDE}/k_{NEP}) for the intramolecular phosphate of **16b**. In other words, the hydrolysis by the intramolecular Zn^{II}−OH^- (**16b**) is 45 000 times faster than by the intermolecular Zn^{II}−OH^- (1 mM **15b**).

The hydrolysis of the phosphoryl intermediate **16** by the intramolecular Zn^{II}−OH^- nucleophile is somewhat analogous to the Lindoy and Sargeson's Co^{III} model system (Scheme 6).[9b] The sigmoidal pH dependence of the hydrolysis rate (pH 6−9) implies the **18a** ⇌ **18b** equilibrium with pK_a of 7.6, and the intramolecular Co^{III}−OH^- nucleophile efficiently attacks the Co^{III}-bound monophosphate with the first-order rate constant of 7.8 × 10^{-4} s^{-1} to form the product **19**.

Summary and Conclusions

The two-step mechanism of phosphate ester hydrolysis by Zn^{II}-containing alkaline phosphatase (AP) (Scheme 1) is well mimicked by the newly designed complex **14**: (i) a phosphoryl intermediate **16** is generated by attack of the hydroxy moiety of the alcohol pendant at the BNP^- (one of the ester group is

concomitantly hydrolyzed) and (ii) the phosphoryl intermediate **16** is hydrolyzed by the intramolecular $Zn^{II}-OH^-$. The attack at the BNP^- substrate and hydrolysis of the intermediate both require Zn^{II}. For the first step, the hydroxyl group is activated by Zn^{II} at physiological pH to **14b** ($pK_a = 7.4$), which is a 125 times more effective nucleophile to the phosphate substrate than the Zn^{II}-activated water of the reference **15b**. For the second step, the intramolecular nucleophile is generated from $Zn^{II}-OH_2$ **16a** with a pK_a value of 9. This intramolecular hydrolysis is 45 000 times faster than the intermolecular hydrolysis of NEP^- with 1 mM **15b**. In the AP enzyme (Scheme 1), these two functions of Zn^{II} are performed separately by two proximate Zn^{II} atoms; one is involved in the activation of Ser-102 to yield phosphoryl intermediate **2**, and the other is involved in the activation of H_2O **3** to attack the intermediate **2**. The intramolecular arrangement of these two Zn^{II} ions in AP is more advantageous than our single-Zn^{II} system in order to provide this dual role, wherein the pK_a value of 9.0 (due to the close phosphate anion or the phosphate-binding) for **16a** $\rightleftharpoons$ **16b** is higher than the reported pK_a value of 7.4 for **2** $\rightleftharpoons$ **3** in the enzyme.

Scheme 4 summarizes the whole reaction mechanism of the P−O bond cleavage of the phosphodiester (BNP^-) by **14**. The final phosphomonoester product **17**, unfortunately, was found to be very inert under normal conditions (all the attempts to hydrolyze it failed, including raising the pH as high as 11). Therefore, we could not use **14** as a catalyst. However, the present results may well serve the novel elucidation of the collaborative roles of Ser-102 and Zn^{II} in alkaline phosphatase.

Experimental Section

General Information. All reagents and solvents used were of analytical grade. The Good's buffers (Dojindo) were commercially available and used without further purification: MES (2-(*N*-morpholino)ethanesulfonic acid, $pK_a = 6.2$), MOPS (3-(*N*-morpholino)propanesulfonic acid, $pK_a = 7.2$), HEPES (*N*-(2-hydroxyethyl)piperazine-*N*′-2-ethanesulfonic acid, $pK_a = 7.6$), EPPS (*N*-(2-hydroxyethyl)piperazine-*N*′-3-propanesulfonic acid, $pK_a = 8.0$), TAPS ((*N*-(tris(hydroxymethyl)methyl)amino)-3-propanesulfonic acid, $pK_a = 8.4$), CHES (2-(cyclohexylamino)ethanesulfonic acid, $pK_a = 9.5$), CAPSO (3-(*N*-cyclohexylamino)-2-hydroxypropanesulfonic acid, $pK_a = 10.0$), CAPS (3-(*N*-cylohexylamino)propanesulfonic acid, $pK_a = 10.4$). Sodium bis-(4-nitrophenyl) phosphate was crystallized from an aqueous solution of bis(4-nitrophenyl) phosphoric acid (BNP) and equimolar NaOH. Lithium ethyl 4-nitrophenyl phosphate was prepared by the reported method.[22] DMF was distilled in vacuo over anhydrous $MgSO_4$ and stored in the dark. All aqueous solutions were prepared using deionized and distilled water.

Kinetic study was carried out using a Hitachi U-3500 spectrophotometer equipped with a thermoelectric cell temperature controller (±0.5 °C). IR spectra were recorded on a Shimadzu FTIR-4200. ^1H (400 MHz), ^{13}C (100 MHz), and ^{31}P (162 MHz) NMR spectra were recorded on a JEOL α-400 spectrometer. 3-(Trimethylsilyl)propionic-*2,2,3,3-d*$_4$ acid sodium salt (Aldrich) in D_2O and tetramethylsilane (Merck) in organic square were used as internal references for ^1H and ^{13}C NMR measurements. A D_2O solution of 80% phosphoric acid was used as an external reference for ^{31}P NMR measurement. Optical rotations were recorded on a Union Giken Automatic Digital Polarimeter PM-101 at 22.0 ± 0.5 °C. Melting points were determined by using a Yanaco micro melting apparatus without any corrections. Elemental analysis was performed on a Yanaco CHN Corder MT-3. Thin layer (TLC) and silica gel column chromatographies were carried out on Merck Art. 5554 (silica gel) TLC plates and Wakogel C-300 (silica gel), respectively.

Synthesis of (*S*)-1-(2-Hydroxy-2-phenylethyl)-1,4,7,10-tetraazacyclododecane (11). 2,6-Dioxo-1,4,7,10-tetraazacyclododecane (**12**) (2.00 g, 10 mmol)[16] and (*S*)-styrene oxide (1.32 g, 11 mmol) were heated to reflux in EtOH (100 mL) for 1 day. The reaction mixture was evaporated to dryness. The residue was purified by silica gel column chromatography (eluent CH_2Cl_2/MeOH/28% aqueous NH_3 = 40:3:0.1) followed by crystallization from CH_3CN to yield 1-(2-hydroxy-2-phenylethyl)-5,9-dioxo-1,4,7,10-tetraazacyclododecane (**13**) as colorless prisms (1.47 g, 4.6 mmol, 46% yield): mp 192.0−193.0 °C; IR (KBr pellet) 3362, 3086, 2975, 2955, 2822, 1655, 1539, 1455, 1435, 1348, 1316, 1291, 1269, 1227, 1200, 1169, 1071, 920, 870, 843, 774, 758, 706 cm^{-1}; TLC (eluent CH_2Cl_2/MeOH/28% aqueous NH_3 = 5:1:0.2) $R_f = 0.4$; ^1H NMR ($CDCl_3$) δ 1.83−2.06 (1H, br, amine NH), 2.51 (2H, dt, $J = 13.2$, 4.6 Hz, NCH), 2.64 (1H, dd, $J = 13.2$, 4.6 Hz, NCH), 2.64 (1H, dd, $J = 13.6$, 4.0 Hz, NCHCPh), 2.77 (2H, ddd, $J = 13.2$, 9.0, 4.2 Hz, NCH), 2.84 (1H, dd, $J = 13.6$, 9.4 Hz, NCHCPh), 3.16−3.24 (1H, br, alcohol OH; 2H, m, CONCH), 3.29 (1H, d, $J = 16.2$ Hz, CHCON), 3.34 (1H, d, $J = 16.2$ Hz, NCOCH), 3.41−3.48 (2H, m, CONCH), 4.79 (1H, dd, $J = 9.4$, 4.0 Hz, CHPh), 7.30 (1H, tt, $J = 6.4$, 2.0 Hz, Ph), 7.35−7.42 (4H, m, Ph), 7.43−7.48 (2H, br, amide NH); $[\alpha]_D$ −55.9° (*c* 1.00, MeOH).

To a suspended solution of dioxo macrocycle **13** (1.92 g, 6.0 mmol) in dry THF (40 mL) was added slowly a THF solution (65 mL) of 1 M BH_3−THF complex at 0 °C. The mixture was stirred at room temperature for 1 h and then heated at 60 °C for 1 day. After decomposition of the excess amount of the hydroborane complex with water at 0 °C, the solvent was evaporated. The residue was dissolved in 6 M aqueous HCl (70 mL) and then the solution was heated at 70 °C for 2 h. The mixture was washed with CH_2Cl_2 (30 mL × 2) and evaporated to dryness. The residue was passed through an anion exchange column of Amberlite IRA-400 with water to obtain **11** as a colorless oil. Crystallization of the oil from 6 M aqueous HCl afforded colorless needles as its tetrahydrochloride salt (**11**·4HCl) in 62% yield (1.63 g, 3.7 mmol): dec 210°; IR (KBr pellet) 3420, 2998, 2793, 2448, 1576, 1495, 1439, 1066, 1028, 766, 704 cm^{-1}; ^1H NMR (D_2O, pD 1.0) δ 2.82−3.21 (18H, m, NCH_2), 4.89 (1H, t, $J = 6.2$, OCHC), 7.40−7.54 (5H, m, ArH); ^{13}C NMR (D_2O, pD 1.0) δ 41.4, 41.5, 44.5, 44.6, 45.4, 47.0, 52.3, 52.4, 62.0, 73.8, 129.0, 131.5, 132.2, 144.8; $[\alpha]_D$ −49.1° (*c* 1.00, H_2O). Anal. Calcd for $C_{16}H_{32}N_4OCl_4 \cdot {}^1/_2H_2O$: C, 43.0; H, 7.44; N, 12.5. Found: C, 43.1; H, 7.49; N, 12.4.

Synthesis of (*S*)-1-(2-Hydroxy-2-phenylethyl)-1,4,7,10-tetraazacyclododecane−Zinc(II) Complex (14a·$(ClO_4)_2$). **11**·4HCl (438 mg, 1.0 mmol) was passed through an anion exchange column of Amberlite IRA-400 with water to obtain the free ligand **11** as a colorless oil. After the oil was dissolved in water (4 mL), $Zn(ClO_4)_2 \cdot 6H_2O$ (391 mg, 1.1 mmol) was added in the solution. The solution was stirred at 60 °C for 1 h. After the solvent was evaporated, the residue was recrystallized from water to obtain colorless prisms as diperchlorate salts **14a**·$(ClO_4)_2$ in 91% yield (507 mg, 0.91 mmol): IR (KBr pellet) 3420, 3293, 2930, 2886, 1480, 1458, 1379, 1365, 1358, 1298, 1283, 1267, 1096, 968, 928, 860, 777, 756, 742, 708, 625 cm^{-1}; ^1H NMR (D_2O, pD 6.0) δ 2.75−3.28 (18H, m, NCH), 5.14 (1H, dd, $J = 10.1$, 3.2 Hz, OCHC), 7.43−7.55 (5H, m, ArH); ^{13}C NMR (D_2O, pD 6.0) δ 45.97, 46.00, 46.2, 48.4, 48.5, 53.7, 55.0, 61.9, 72.4, 128.9, 131.4, 131.8, 114.0; $[\alpha]_D$ −64.4° (*c* 1.00, H_2O). Anal. Calcd for $C_{16}H_{28}N_4O_9Cl_2Zn$: C, 34.5; H, 5.1; N, 10.1. Found: C, 34.7; H, 5.2; N, 10.0.

Preparation of Alkoxide Pendant Attached Zinc(II) Complex with 11 (14b·ClO_4). To a solution of **14a**·$(ClO_4)_2$ (278 mg, 0.50 mmol) in MeOH (11 mL) was added 0.5 mL of 1 M methanolic NaOMe. Colorless solid was precipitated by slow evaporation and recrystallized from aqueous solution (pH 9.5) to obtain **14b**·ClO_4 as colorless prisms in 96% yield (219 mg, 0.48 mmol): IR (KBr pellet) 3295, 2922, 2874, 1489, 1453, 1350, 1144, 1094, 982, 932, 855, 795, 774, 756, 710, 625 cm^{-1}; ^1H NMR (D_2O, pD 9.5) δ 2.69−3.09 (17H, m, NCH_2), 3.22 (1H, ddd, $J = 13.8$, 11.1, 4.3 Hz, NCH_2), 4.86 (1H, t, $J = 6.6$ Hz, OCHC), 7.34−7.49 (5H, m, ArH); ^{13}C NMR (D_2O, pD 9.5) δ 45.2, 46.2, 46.6, 46.8, 47.6, 48.1, 52.6, 54.9, 63.5, 74.3, 129.2, 130.8, 131.6, 146.0; $[\alpha]_D$ −65.8° (*c* 1.00, H_2O). Anal. Calcd for $C_{16}H_{27}N_4O_5ClZn$: C, 42.1; H, 6.0; N, 12.3. Found: C, 42.4; H, 6.0; N, 12.2.

Synthesis of (*S*)-1-(2-(4-Nitrophenylphosphoryl)-2-phenylethyl)-1,4,7,10-tetraazacyclododecane (16a·ClO_4). A DMF solution (8 mL) of **14b**·ClO_4 (91.3 mg, 0.20 mmol) and bis(4-nitrophenyl) phosphate sodium salt (72.4 mg, 0.20 mmol) was stirred at 35 °C for 1 day. After the solvent was evaporated, the residue was dissolved in water (50 mL) and the pH was adjusted to 6.0 with 0.1 M aqueous $HClO_4$. The aqueous solution was washed with diethyl ether (15 mL × 3) and

(22) (a) Morrow, J. R.; Trogler, W. C. *Inorg. Chem.* **1988**, *27*, 3387−3394. (b) Kirby, A. J.; Younas, M. *J. Chem. Soc. B* **1970**, 1165−1172.

evaporated to dryness. The residue was recrystallized from water to obtain **16a**·ClO_4 as colorless prisms (98 mg, 0.15 mmol, 73% yield): dec 175°; IR (KBr pellet) 3303, 2934, 2885, 1611, 1591, 1514, 1493, 1458, 1346, 1252, 1146, 1090, 916, 864, 793, 754, 741, 700, 625, 550 cm^{-1}; ^1H NMR (D_2O, pD 6.5) δ 2.93−3.30 (17H, m NCH_2), 3.37 (1H, dd, J = 15.3, 9.8 Hz, NCH_2), 5.47 (1H, m, OCH), 7.02 (2H, dtd, J = 9.3, 2.0, 0.9 Hz, $OArHNO_2$), 7.33−7.46 (5H, m, CArH), 8.05 (1H, dtd, J = 9.3, 2.0, 0.6 Hz, $OArNO_2$); ^{13}C NMR (D_2O, pD 6.5) δ 45.6, 45.7, 46.9, 47.0, 47.8, 47.9, 53.3, 56.7, 65.1 (J_{PC} = 5.9 Hz), 80.2 (J_{PC} = 6.6 Hz), 123.0 (J_{PC} = 5.1 Hz), 128.4, 129.1, 131.6, 131.7, 140.3, 146.5, 159.0 (J_{PC} = 5.9 Hz); ^{31}P NMR (D_2O, pD 6.5) δ −3.59 (J_{HP} = 9.2, 2.7 Hz); $[\alpha]_D$ −43.2° (c 1.00, MeOH). Anal. Calcd for $C_{22}H_{33}N_5O_{11}ClPZn$: C, 39.1; H, 4.9; N, 10.4. Found: C, 38.9; H, 4.9; N, 10.4.

Syntheses of Racemic Ligand and Its Zn^{II} Complexes. The racemic dioxocyclen derivative was prepared by the same method as that for **13** using *rac*-styrene oxide to give colorless prisms in 43% yield. Mp, TLC, IR, and NMR are the same as those for **13**.

Using this dioxocyclen derivative, the racemic ligand (cyclen derivative) was prepared by the same method as **11** to give colorless needles as its tetrahydrochloric acid salts in 60% yield. Dec, IR, and NMR are the same as those for **11**·4HCl. $[\alpha]_D$ = 0° (c 1.00, H_2O). Anal. Calcd for $C_{16}H_{32}N_4OCl_4 \cdot {}^1/_2H_2O$: C, 43.0; H, 7.44; N, 12.5. Found: C, 43.0; H, 7.41; N, 12.1.

The pendant alcohol undissociated Zn^{II} complex with the racemic ligand was prepared by the same method as that for **14a** using the racemic ligand to give colorless prisms as its diperchlorate salts in 93% yield. IR and NMR are the same as those for **14a**·$(ClO_4)_2$. $[\alpha]_D$ = 0° (c 1.00, H_2). Anal. Calcd for $C_{16}H_{28}N_4O_9Cl_2Zn$: C, 34.5; H, 5.1; N, 10.1. Found: C, 34.8; H, 5.2; N, 10.1.

Using this Zn^{II} complex, the alkoxide pendant attached Zn^{II} complex was prepared with the same method as that for **14b** to give colorless prisms as perchlorate salts in 90% yield. IR and NMR are the same as those for **14b**·ClO_4. $[\alpha]_D$ = 0° (c 1.00, H_2O). Anal. Calcd for $C_{16}H_{27}N_4O_5ClZn$: C, 42.1; H, 6.0; N, 12.3. Found: C, 42.0; H, 6.3; N, 12.3.

Crystallographic Study. A colorless prismatic crystal of **14b**·ClO_4 (0.40 × 0.40 × 0.20 mm) was used for data collection. The lattice parameters and intensity data were measured on a Rigaku AFC7R diffractometer with graphite-monochromated Cu Kα radiation and a 12-kW rotating anode generator. The structure was solved by a Patterson orientation/translation search and expanded using Fourier techniques. The non-hydrogen atoms were refined ansiotropically. Hydrogen atoms were included but not refined. The final cycle of full-matrix least-squares refinement was based on 2862 observed reflections ($I > 3.00\sigma(I)$) to give R = 0.050 and R_w = 0.077. All calculations were performed using the teXsan crystal structure analysis package developed by Molecular Structure Corp. (1985 and 1992).

Potentiometric pH Titration. The preparation of the test solutions and the calibration method of the electrode system were described earlier.[10,13] All test solutions (50 mL) were kept under an argon (>99.999% purity) atmosphere at 25.0 ± 0.1 °C with I = 0.10 ($NaClO_4$) and 35 ± 0.1 °C with I = 0.10 ($NaNO_3$). The potentiometric pH titrations were carried out at [total ligand] = 1 mM in the presence or absence of equimolar $ZnSO_4$, and [total Zn^{II} complex] = 1 mM, and at least three independent titration were made. The calculation methods for ligand protonation constants (K_n), Zn^{II} complexation constants (K(ZnL)), and the deprotonation constant of the Zn^{II} complex (K_a) were the same as described previously.[10,13] The protonation constants K_n are defined as $[H_nL]/[H_{n-1}L]a_{H^+}$, the 1:1 metal complexation constant K(ZnL) as $[ZnL]/[Zn^{II}][L]$, and the deprotonation constant K_a as $[ZnH_{-1}L]a_{H^+}/[ZnL]$. The used values of K_w' (= $[H^+][OH^-]$) and f_{H^+} were $10^{-13.79}$ and 0.825 at 25 °C and $10^{-13.48}$ and 0.823 at 35 °C, respectively.

Kinetics Procedure for the Phosphodiester Cleavage Reaction with Zinc(II) Complexes in Aqueous Solution. The phosphodiester cleavage reaction (i.e., 4-nitrophenolate release reaction) rates of bis(4-nitrophenyl) phosphate (BNP^-) and ethyl 4-nitrophenyl phosphate (NEP^-) were measured by an initial slope method (following the increase in 400-nm absorption of released 4-nitrophenolate) in aqueous solution at 35.0 ± 0.5 °C. Buffer solutions containing 20 mM Good's buffer (MES, pH 6.0; MOPS, pH 7.0; HEPES, pH 7.4; EPPS, pH 7.9; TAPS, pH 8.4; CHES, pH 9.3; CAPSO, pH 10.0) were used, and the ionic strength was adjusted to 0.10 with $NaNO_3$ (ca. 90 mM). For the initial rate determination, the following typical procedure was employed: BNP^- (10, 5.0, and 2.5 mM) and **14b** (2.0, 1.0, and 0.50 mM) were mixed in the buffered solution, the UV absorption increase recorded immediately and then followed generally until ca. 0.1% formation of 4-nitrophenolate, where log ϵ values for 4-nitrophenolate were 3.23 (pH 6.0), 3.94 (pH 7.0), 4.11 (pH 7.4), 4.20 (pH 7.9), 4.24 (pH 8.4), 4.26 (pH 9.3), and 4.26 (pH 10.0) at 400 nm. The observed first-order rate constant k_{obsd} (s^{-1}) was calculated from the decay slop (4-nitrophenolate release rate/[BNP^-]). The value of k_{obsd}/[total Zn^{II} complex] gave the second-order rate constant k'_{BNP} (M^{-1} s^{-1}) for BNP^- hydrolysis. The second-order rate constant k_{BNP} was determined from the maximum k'_{BNP} values.

The second-order rate constants, k_{BNP} and k_{NEP}, for Zn^{II}–*N*-methylcyclen **15b** were determined by the same method for that for **14b** with BNP^- (10, 5.0, and 2.5 mM) and **15b** (16, 8.0, and 4.0 mM) and NEP^- (20, 10, and 5.0 mM) and **15b** (20, 10, and 5.0 mM), respectively.

Kinetics Procedure for the Phosphodiester Cleavage Reaction with 14b in DMF. The phosphodiester cleavage rate of bis(4-nitrophenyl) phosphate (BNP^-) was measured by an initial slope method (following the increase in 430-nm absorption of released 4-nitrophenolate) in DMF at 35.0 ± 0.5 °C. For the initial rate determination, the following procedure was employed: BNP^- (1.0, 0.50, and 0.25 mM) and **14b** (0.20, 0.10, and 0.050 mM) were mixed in DMF, the UV absorption increase recorded immediately and then followed generally until ca. 1% formation of 4-nitrophenolate, where log ϵ of 4-nitrophenolate was 4.45 at 430 nm. The second-order rate constant k_{BNP} in DMF was determined by the similar method for k_{BNP} in aqueous solution.

Kinetics Procedure for Intramolecular Hydrolysis with 16b. The hydrolysis (i.e., 4-nitrophenolate release reaction) rate of **16b** was measured by an initial slope method (following the increase in 400-nm absorption of released 4-nitrophenolate) in aqueous solution at 35.0 ± 0.5 °C. Buffer solutions containing 20 mM Good's buffer (HEPES, pH 7.4; EPPS, pH 7.9; TAPS, pH 8.3 and 8.6; CHES, pH 9.1 and 9.5; CAPSO, pH 10.0; CAPS, pH 10.5) were used, and the ionic strength was adjusted to 0.10 with $NaNO_3$ (ca. 90 mM). For the initial rate determination, the following procedure was employed: **16b** (1.0, 0.50, and 0.25 mM) were mixed in the buffered solution, the UV absorption increase recorded immediately and then followed generally until ca. 1% formation of 4-nitrophenolate, where log ϵ values of 4-nitrophenolate were 4.11 (pH 7.4), 4.24 (pH 8.3), 4.25 (pH 8.6), 4.26 (pH 9.1), 4.26 (pH 9.5), 4.26 (pH 10.0), and 4.27 (pH 10.5). The first-order rate constant k'_{PDE} (s^{-1}) was calculated from the decay slop. The first-order rate constant k_{PDE} (s^{-1}) was obtained from the maximum k'_{PDE}.

Acknowledgment. We are thankful to the Ministry of Education, Science and Culture in Japan for financial support by a Grant-in Aid for Science Research (A) (No. 04403024) for E.K. and by a Grant-in-Aid for Encouragement of Young Scientists (No. 06857180) for T.K. NMR instruments in the Research Center for Molecular Medicine (RCMM) in Hiroshima University were used.

Supporting Information Available: Text describing experimental details for crystallographic study, and listsings of crystallographic parameters, atomic coordinates, anisotropic displacement parameters, bond lengths, bond angles, torsion angles, and nonbonded contacts for **14b**·ClO_4 (30 pages); listing of observed and calculated structure factors for **14b**·ClO_4 (20 pages). This material is contained in many libraries on microfiche, immediately follows this article in the microfilm version of the journal, can be ordered from the ACS, and can be downloaded from the Internet; see any current masthead page for ordering information and Internet access instructions.

JA951008P